Melt Dynamics and Hole Formation during Drilling with Ultrashort Pulses

Andreas MICHALOWSKI[*], Dmitrij WALTER[**], Friedrich DAUSINGER[*,**] and Thomas GRAF[*,**]

[*] *Institut für Strahlwerkzeuge (IFSW),Universität Stuttgart, Germany*
michalowski@ifsw.uni-stuttgart.de
[**] *Forschungsgesellschaft für Strahlwerkzeuge mbH (FGSW), Pfaffenwaldring 43, 70569 Stuttgart, Germany*

Drilling with ultrashort laser pulses is a suitable technique for the production of micro-holes with high aspect ratios. For best quality an appropriate drilling strategy, e. g. helical drilling, has to be applied. The reasons for improved hole quality compared to percussion drilling are investigated. Melt transport is studied using special sandwich samples consisting of iron and nickel layers. Spatially resolved EDX analysis of the deposited melt helps to estimate the mechanism of melt transport. It seems that the melt expulsion at the beginning of the process which is responsible for the burr formation is more efficient in the case of percussion drilling than for helical drilling. The quality advantages of helical drilling are assumed to result from a different hole geometry during processing.

DOI: 10.2961/jlmn.2008.03.0015

Keywords: melt dynamics, helical drilling, percussion drilling, hole formation, burr formation

1. Introduction

Different applications of holes drilled in metals by lasers are in need of different laser sources and processing strategies. If highest productivity is required, single pulse drilling with long pulse durations and high pulse energies is common. In this case the material removal is nearly completely dominated by melt ejection [1,2]. For holes with highest quality in terms of sharp edges, no burr and essentially no melt deposition, a reduction of fluence and pulse duration to the ns or even ultrashort regime (ps, fs) is beneficial [3,4]. Furthermore an adequate drilling strategy can also improve the quality. Helical drilling for instance generates better results than percussion drilling [5]. On the other hand, the number of pulses which are needed to complete the drilling process increases which is counterproductive in industrial applications. Further advances in optimizing the drilling process need a better understanding of the melt dynamics and the formation of holes.

The melt and the vapor are produced at the bottom of the blind hole during processing and are accelerated in the direction of the entrance. Depending on drilling phase and process dynamics the molten material is ejected from the hole, forms a burr or deposits at the walls. If the deposition is not removed by later pulses the achieved quality is reduced. From this point of view it is clear that a reduction of fluence and pulse duration is advantageous because the amount of molten material is decreased [3]. Apparently the maximum distance the melt can move before solidification can be important for the achieved quality. To observe this maximum distance, special "sandwich samples" composed of iron and thin nickel layers have been drilled and analyzed. Nickel and iron were chosen because of their similar physical properties (Table 1).

Energy dispersive X-ray analysis (EDX) was applied to estimate the amount of nickel inside the deposited layers at different depths from the surface.

Different hole-shapes were observed before the end of the process in a comparison of percussion drilling and helical drilling. In the following a simple model of beam propagation inside the hole is presented which can qualitatively explain this differences.

Table 1 Physical properties of sandwich materials

Parameter	Iron	Nickel	Unit
Density	7.87	8.9	g/cm^3
Melting point	1808	1726	K
Heat of fusion	13.8	17.2	kJ/mol
Boiling point	3023	3005	K
Heat of vaporization	349.5	377.5	kJ/mol
Thermal conductivity	80.2	90.7	W/mK
Heat capacity	0.449	0.444	J/g K

2. Experimental procedure

Several holes have been drilled in 1 mm thick sandwich samples by percussion and helical drilling with a Ti:Sapphire laser at 1 kHz. The parameters are summarized in Table 2. A scanner was used for beam deflection. It was turned off for percussion drilling. Various numbers of pulses have been used to produce blind holes as well as through holes. Two samples with Ni layers in 500 µm and 900 µm depth respectively have been used. The thickness of the Ni layer inside the sandwich was 100 µm in both cases. Each sample was drilled with percussion and helical drilling strategy. After processing, the samples were cut, grinded and polished to study the melt deposition at the

walls. Because of the very brittle deposited melt layer ultrasonic cleaning was not possible.

The melt layer was analyzed at several depths inside the hole with spatially resolved EDX analysis. It turned out that the concentration of oxygen decreases strongly at the transition from the recast layer to the bulk material and is therefore a good indicator to measure the thickness of the melt deposition.

Table 2 Processing parameters

Parameter	Value
F	≈ 225 J/cm^2
τ_P	5 ps
f	80 mm
d_f	15 µm
z_f	-100 µm
M^2	≈ 1.7
$d_{\text{Helical Path}}$	20 µm

3. Results

The used fluence of 225 J/cm^2 generates very thick recast layers. These layers were necessary for the analysis of melt transport. As expected the cylindricity of the holes created with helical drilling was much better than in the case of percussion drilling. But contrary to the expectations the recast layer in the region of the entrance was more pronounced for helical drilling (Fig. 1). As seen from Fig. 1 the melt distribution at depths from 350 µm to 1000 µm is very similar for both drilling strategies. It is also found that the measured melt layer thickness first increases from the surface to a depth of approximately 300 µm and decreases at higher depths.

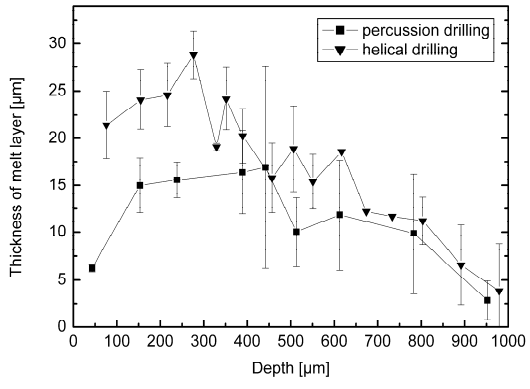

Fig. 1 Thickness of deposit layer

For a sample with the Ni-layer at a depth of 500 µm Fig. 2 and Fig. 3 show the measured fraction of Ni inside the melt deposition for percussion and helical drilling respectively. No Ni was detected at depths exceeding 500 µm (i.e. deeper than the Ni-layer). This proves that the transport of molten material is only directed upwards to the entrance of the hole. This result is certainly expected for blind holes because without an exit at the bottom the pressure caused by the laser pulse can only escape through the hole-entrance. But also in through holes no nickel was found below the Ni-layer.

Fig. 2 and Fig. 3 show a strong difference in the amount of Ni distribution inside the layer between both drilling strategies. The amount of Ni inside the deposition is significantly smaller in the case of percussion drilling and decreases not as explicitly as for helical drilling. Evidently the melt expulsion of the molten material is more efficient for percussion drilling during the first phase of drilling. This is in agreement with the result that less deposition was found in this region for percussion drilling. In the case of helical drilling most of the molten material seems to remain near the place of formation. In section 4 a possible explanation is given for this finding.

Similar results were found with the Ni-layer at a depth of 900 µm (see Fig. 4 and Fig. 5). Starting at a depth of 900 µm the melt seems to move a larger distance during percussion drilling than in the case of helical drilling but the difference is not as pronounced as discussed before. It seems that the melt produced in this depth can hardly leave the hole because only little Ni was found inside the layer near the entrance. From these results it can be estimated that from this depth the melt moves a distance of 600 µm and 400 µm for percussion and helical drilling, respectively.

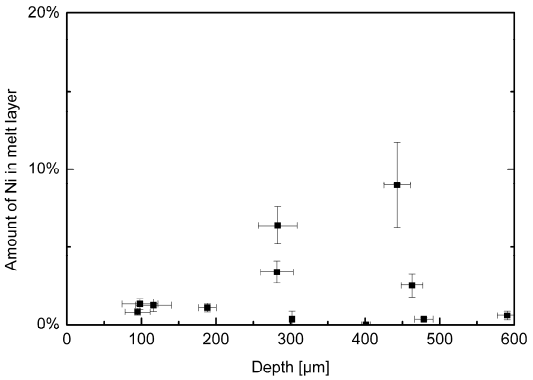

Fig. 2 Amount of Ni inside the deposit layer for percussion drilling. The Ni layer was located at a depth of 500 µm.

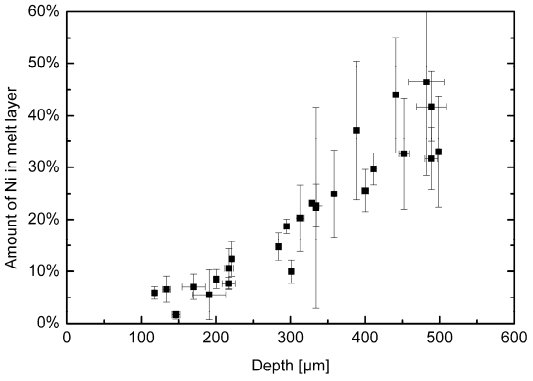

Fig. 3 Amount of Ni inside the deposit layer for helical drilling. The Ni layer was located at a depth of 500 µm.

4. Hole formation

To understand the differences in melt movement it is interesting to observe the differences of the hole formation between both drilling processes. During the first drilling phase when hole depths are small the averaged fluence with regard to one rotation on the helical drilling path differs strongly from percussion drilling (Fig. 6). This results in a larger inlet aperture for helical drilling during this phase. In contrast the percussion drilling process starts with a narrower channel and a pronounced tip. This difference in geometry is maintained during the whole drilling process as illustrated by the blind holes shown in Fig. 7 and Fig. 8 for percussion and helical drilling, respectively. From this point of view it can be understood that the melt ejection process is more efficient for percussion drilling than for helical drilling.

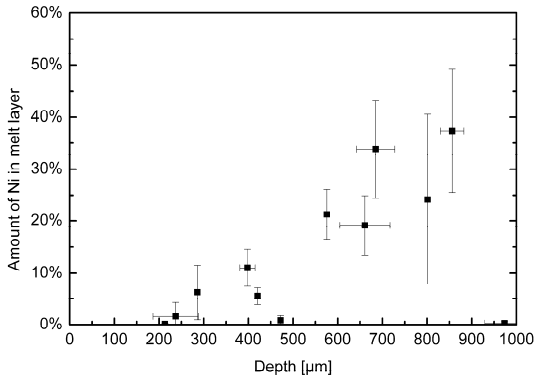

Fig. 4 Amount of Ni inside the deposit layer for percussion drilling. The Ni layer was located at a depth of 900 µm.

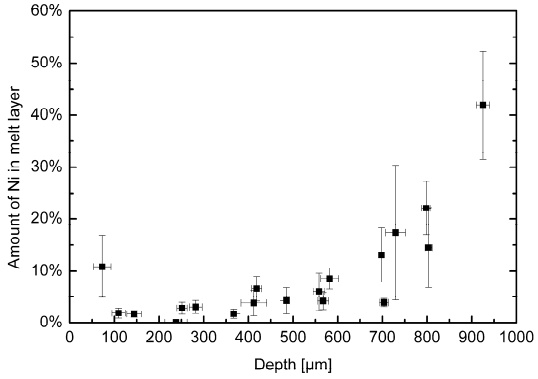

Fig. 5 Amount of Ni inside the deposit layer for helical drilling. The Ni layer was located at a depth of 900 µm.

The pressure caused by the material ablation can only blow out through the narrow channel and the melt will be accelerated more effectively than in case of the wider channel generated with helical drilling. This assumption is supported by the experimental results shown in Fig. 2 and Fig. 3. The melt seems to be ejected much more efficiently in case of percussion drilling.

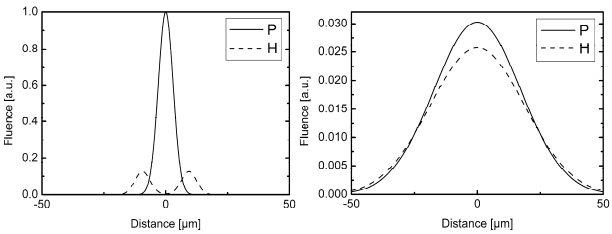

Fig. 6 Averaged fluences of percussion drilling (P) and helical drilling (H) at the positions z = 0 µm (left) and z = -400 µm (right).

If the channel is too deep no molten material can leave the hole any more except in form of droplets. This assumption is also supported by the observation of the development of the burr height during drilling of steel (Fig. 9). The material ejected from the hole forms a burr at the surface, which is observed only during the first phase of drilling. When the melt expulsion stops the burr is partially ablated by the following pulses.

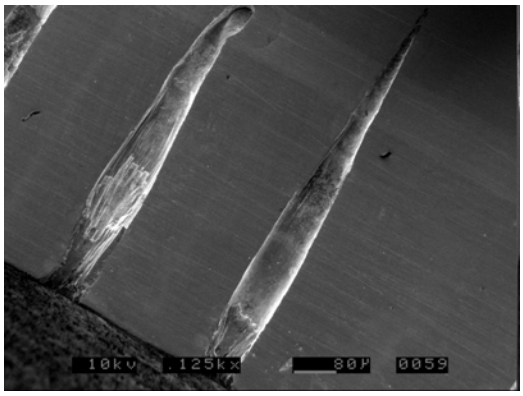

Fig. 7 Percussion drilled blind holes after 15000 pulses. The channel is narrow and shows a pronounced tip.

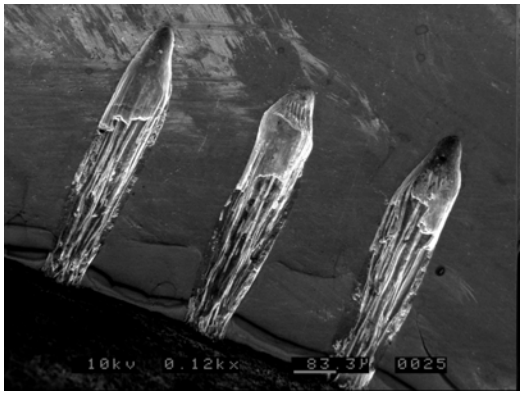

Fig. 8 Helically drilled blind holes after 40000 pulses. The channels are nearly cylindrical and show a rounded tip at this phase.

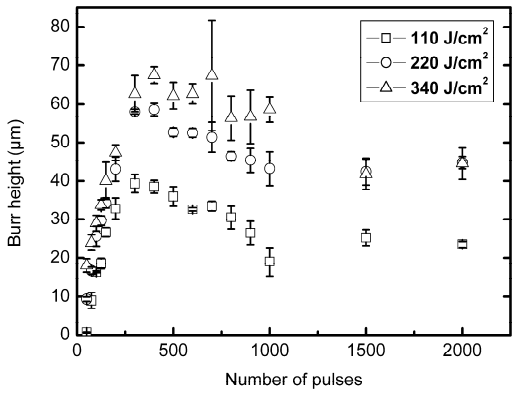

Fig. 9 Burr development during percussion drilling of steel. The maximum burr height increases with fluence. The burr is partly ablated at later drilling phases.

By comparing percussion and helical drilling the differences of laser intensity distribution diminish during free beam propagation (Fig. 6). But with increasing hole depth the reflection of the laser beam at the wall gains importance. This effect is expected to cause a change of intensity distribution compared to propagation in free space.

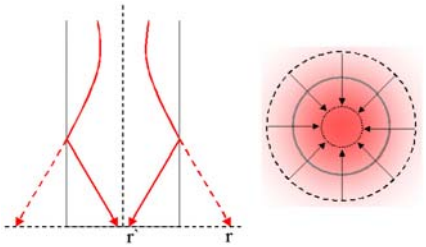

Fig. 10 To calculate the intensity distribution the beam was freely propagated to the ground plane (dotted line). The intensity distribution outside the cylinder was folded afterwards to the inside.

As a first approximation the hole geometry is assumed to be perfectly cylindrical. The resulting intensity distribution consists of two parts if only one single reflection is taken into account, namely the freely propagated and the one time reflected fraction. This calculation can easily be done by ray tracing and is sketched by Fig. 10. In case of percussion drilling the calculation can easily be done analytically. Taking only single reflections into account the sum intensity at the ground is found to be

$$F_1(r) = f(r) + \frac{2R-r}{r} f(2R-r) + \frac{2R+r}{r} f(2R+r).$$

In this formula f(r) denotes a radially symmetric intensity distribution in the target plane calculated assuming free-space beam propagation and R the radius of the cylinder. It is obvious that this formula is only an approximation because the resulting intensity distribution $F_1(r)$ shows a singularity at $r = 0$. This is because geometrical optics does not take into account diffraction effects. But this results in high intensities that can be generated in the center of the hole due to reflections at the hole wall. This effect might be responsible for the pronounced and narrow tip which is obtained during percussion drilling (Fig. 7).

In the case of helical drilling the calculation based on the same method was done numerically. Since the incident beam is not centered in this case no symmetric analytical formula can be derived. Again intensity peaks appear near the center of the cylinder due to focusing caused by the cylindrical walls. For the parameters of the calculation which are the same as summarized in Table 2 selected results are shown in Fig. 11 . The beam intensity distribution was assumed to be Gaussian and the diameter of the hole was fixed to 60 µm. With increasing hole-depth the intensity peaks near the center become more and more pronounced.

From this model it is expected that at a certain depth of the hole a tip is formed also for helical drilling. Indeed the tip of helically drilled blind holes becomes narrower and longer for large channel depths. Fig. 12 shows a tip which was obtained by helical drilling. Inside such a tip the reflection will most likely again lead to the hole focusing effect described above. Since the averaged fluence distribution over one turn becomes similar to percussion drilling (Fig. 6) it is expected that this tip again becomes more and more pronounced for deep holes far from the beam waist. Indeed this is observed for helical drilling of steel (Fig. 13). This means that the differences between percussion drilling and helical drilling vanish for increasing channel depth. This is in agreement with the experimental result that the maximum distance the melt can rise inside the hole becomes similar for percussion drilling and helical drilling (Fig. 4 and Fig. 5).

5. Summary and Conclusions

Melt dynamics and hole formation was studied in the case of drilling with ultrashort laser pulses using samples consisting of layers of iron and nickel. Spatially resolved EDX analysis gives the possibility to study the distance the melt can rise above the place of generation. It was shown that the melt expulsion at the beginning of the drilling process is more efficient for percussion drilling than for helical drilling. The expulsed material forms a burr at the entrance of the work piece. If the channel is deep enough the melt cannot leave the hole any more and the burr height can slightly decrease because of ablation due to the following pulses.

The hole geometry achieved with percussion drilling differs significantly from helical drilling at the beginning of the process. Holes drilled with percussion drilling are narrow at the beginning and show a pronounced tip. In contrast to this the channel obtained by helical drilling at the beginning of the process is much broader at the entrance and shows a rounded tip. This can be explained with different averaged fluence distributions near the beam waist. Reflections at the hole walls lead to a focusing effect which induces that the channel remains narrow and peaked during percussion drilling. In contrast the hole geometry obtained with helical drilling is already nearly cylindrical during this phase. For increasing channel depth the differences between percussion drilling and helical drilling diminish.

The maximum rising distance of the melt which is produced in a depth of 900 µm was found to be similar for both processes. It was also observed, that even for helical drilling a tip is formed in the deep channels. A possible

explanation are reflections at the walls which can lead to high fluences in the center of the hole.

Since the quality of holes drilled with helical drilling is higher than for percussion drilling the differences between the two strategies should be maintained as long as possible during processing. This means that a large Rayleigh length and a small focus is beneficial for the hole quality. This can be achieved by using a good beam quality and short laser wavelengths.

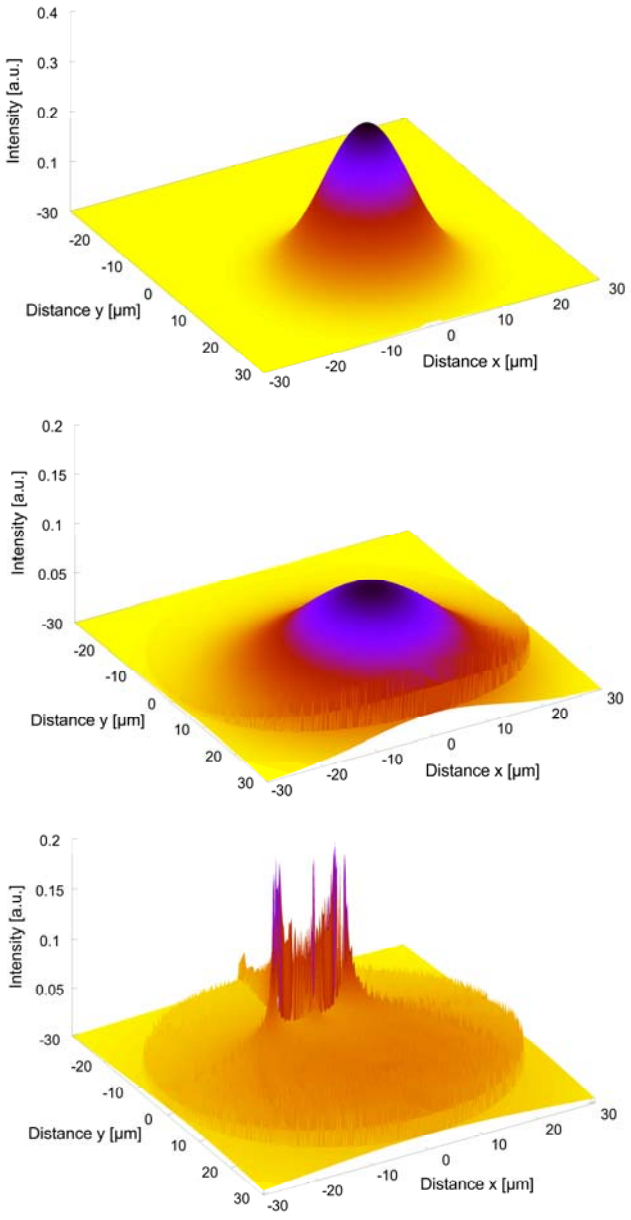

Fig. 11 Expected intensity distributions for helical drilling due to reflections at the hole wall for distances from the beam waist of 200 µm, 400 µm and 800 µm. The calculation was done with ray tracing.

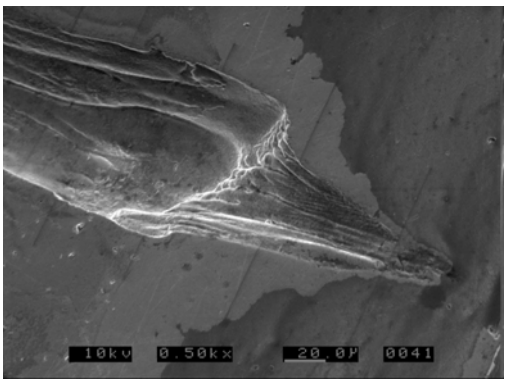

Fig. 12 Tip of blind hole during helical drilling

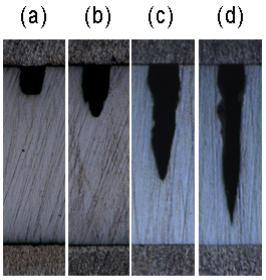

Fig. 13 Change of hole geometry during helical drilling of 1 mm steel. For increasing hole depth a sharp tip appears. Depths are 160 µm (a), 280 µm (b), 540 µm (c) and 840 µm (d).

Acknowledgments

The authors gratefully acknowledge the Deutsche Forschungsgemeinschaft (DFG) for financial support. This work is part of the DFG project DA 335/5 which is part of the SPP 1139.

References

[1] K. T. Voisey, C. F. Cheng and T. W. Clyne: "*Laser-Solid Interactions for Materials Processing"*, ed. by D. Kumar, D. P., Norton, C. B. Lee, K. Ebihara and X. Xi, Vol. 617, San Francisco, (2000), Paper J5.6.

[2] L. Trippe, J. W. Willach, E. W. Kreutz, W. Schulz, J. Petereit, S. Kaierle, R. Poprawe: Proc. Fifth International Symposium on Laser Precision Microfabrication, Nara (Japan), (2004) p. 609 – 615.

[3] A. Ruf: „Modellierung des Perkussionsbohrens von Metallen mit kurz- und ultrakurz gepulsten Lasern", Herbert Utz Verlag, München, (2004).

[4] D. Breitling, C. Föhl, F. Dausinger, T. Kononenko, V. Konov: „Femtosecond Technology for Technical and Medical Applications", ed. by F. Dausinger, F. Lichtner, H. Lubatschowski, Topics Appl. Phys. 96, Springer-Verlag Berlin Heidelberg, (2004), p. 131-156.

[5] C. Föhl, D. Breitling, F. Dausinger: Proc. 21th International Congress on Applications of Lasers & Electro – Optics ICALEO, (2002).

(Received: May 12, 2007, Accepted: March 24, 2008)